Strategy for Power Quality Improvement and Maximum Demand Smoothing

Willy M. Siti Adisa A. Jimoh Dan V. Nicolae
Tshwane University of Technology
Private Bag 0X 017, 0116, Pretoria North
SOUTH AFRICA
willysiti@yahoo.com jimohaa@tut.ac.za danaurel@yebo.co.za

Abstract – **In this paper, a distributed strategy for improving the power quality and maximum demand smoothing is presented. Many authors have presented the power quality improvement as a centralized issue, which implies high power capability of compensators. Based on multi-functionality of specific switching-mode converters, a decentralised model is presented. A discussion of simultaneity of different functions is presented in details. The results of this paper are intended to be a guideline for application designers.**

I. INTRODUCTION

Power quality events such as voltage sags, swells, switching transients, notches, flickers and harmonics have become far more problematic. This is because of the increased use of sensitive electronic loads like variable speed drives and computers [1]-[4]. To improve the immunity or ride through ability of the sensitive equipment to these events, the shape of the current supply should be improved [5]-[7]. This paper introduces a power electronic switching strategies aimed at solving power quality problems at any plant.

In order to address the power quality a multi-purpose switching mode converter [8], [10] as front-end stage of other independent equipment was used. The same front-end stage, with a minimum change in control, can also be used as maximum power demand smoothing.

II. PROPOSED MODEL

A common strategy for improving power quality of a company, and achieving harmonic and reactive compensation, is as a centralized unit. Figure 1 shows such a strategy where $DB_{1...n}$ represent distribution boxes and PQC represents one centralized power quality compensator.

In plants/companies where the installed power is high, this solution results in high power capability PQC. The real problem, however, with a large central PQC device is that the power quality at any consumer depends on the proximity of distorting loads and the PQC device. Consequently, effectiveness of power quality compensation is not the same for the plants. Though debatable, there is also the question of cost effectiveness of a centralized unit as opposed to a distributed one. As well a centralized unit being only one point of compensation, entire effort depends on the reliability of this only one PQC.

The distributed concept studied in this paper and shown in figure 2 tries to address the main drawbacks of the centralized solution. Any small system supplied from a distribution box can contain, or can be designed to have, at least equipment, such as UPS, AC or DC drive, battery charger, or DC power supply.

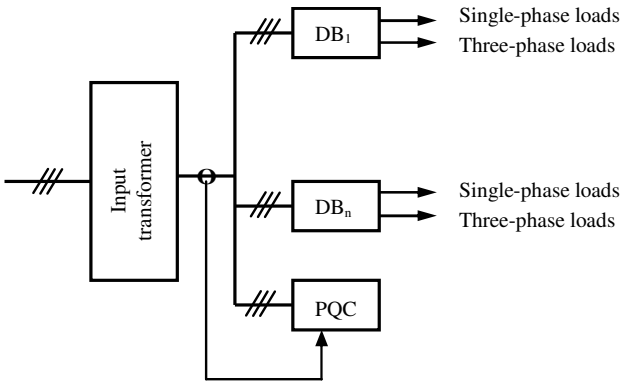

Fig. 1. Centralised strategy of PQC

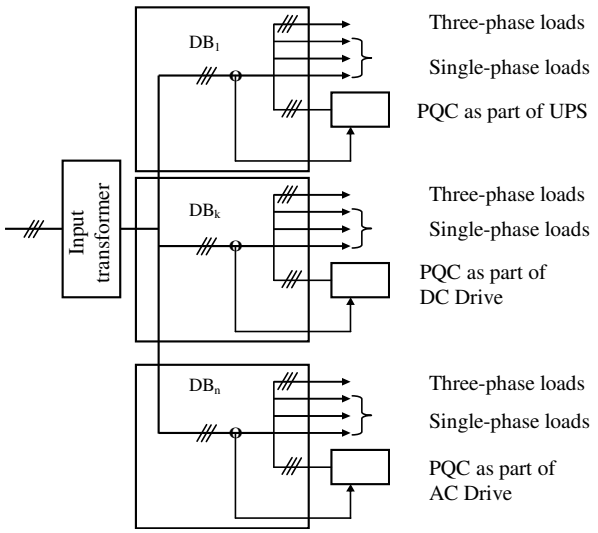

Fig. 2 Distributed strategy of PQC

As front-end stage ac-to-dc converter a boost switching-mode converter with classic three-arm ***H*** topology should be used, see figure 3. In this figure, $[v_s]$ is the matrix of supply voltage, $[i_s]$ – the current delivered by the source (in this situation the distribution box), $[i_L]$ – all the other currents delivered from that DB considered as non-linear (in this non-linearity all perturbation such as phase-shift, harmonic distortion and unbalancing are included), $[i_c]$ – the input current into converter, I_d – the output current from the converter, I_o – the DC current delivered to the equipment (UPS, AC/DC drive, battery charger or any DC load), R_{in} – the voltage input adapter, R_o – the output voltage adapter,

$G_{1...6}$ – the gate signal controls, L – the input inductor (one for each phase) and C – the storage capacitor.

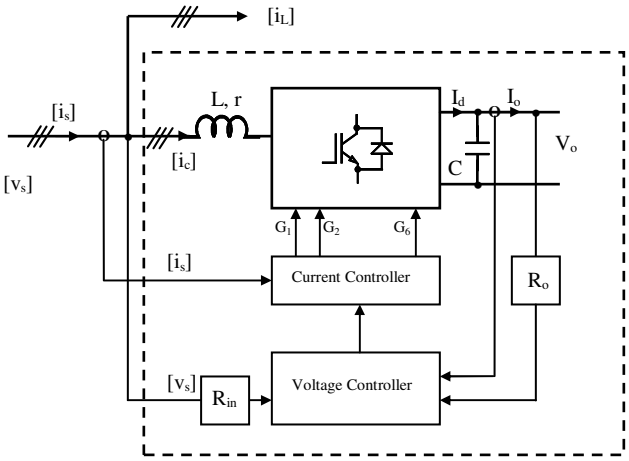

Fig. 3 Front end stage with PQC capability

The current controller used in this study is a hysteresis-type with limiter and control of the highest switching frequency [9], which forces the current to follow the shape of the reference.

The voltage controller has the task of maintaining constant dc bus during power quality compensation. When the quasi-sinusoidal inverter function is requested in order to smooth the maximum demand, then the ties of the voltage controller with the dc bus are broken. A battery is coupled to the dc bus and a lag compensator compares the voltage at the point of common connection (PCC) with a reference creating the reference for the current controller. A small capacitor is introduced in parallel at PCC in order to attenuate the switching frequency influence.

III. POWER BALANCE PRINCIPLE

This analysis is intended to clarify the power exchange between the supply, non-linear load and the converter while it performs simultaneous functions of unity power factor rectification (UPFR) – as the main function, reactive power compensation, harmonic compensation (active power filter APF and unbalancing correction. Throughout the analysis the AC bus will be considered to be infinite and no voltage distortion is taking place. Neglecting the losses of the ***H*** converter, the relation between the instantaneous powers delivered by the supply (p_s) the instantaneous power drawn by the non-linear load (p_L) and the switching-mode converter (p_c) can be written as:

$$p_s = p_L + p_c \tag{1}$$

The parameters of the supply are:

$$[v_s]^t = \sqrt{2} \times V_s \sin\left[\omega t - \frac{2\pi}{3}(i-1)\right] \tag{2}$$

with i=1,2,3

$$[i_s]^t = \sqrt{2} \times I_s \sin\left[\omega t - \frac{2\pi}{3}(i-1)\right] \tag{3}$$

with i = 1,2,3

Where V_s and I_s are the rms value of the supply voltage and current respectively.

$$[i_L]^t = \sum_{h=1}^{\infty} \sqrt{2} \times I_L \sin\left[h \times \left(\omega t - \frac{2\pi}{3}(i-1)\right) - \varphi_h\right] \tag{4}$$

$$p_L = [v_s]^t \cdot [i_L] = 3 \cdot V_s \cdot I_{L1} \cdot \cos\varphi_1 + \sum_{h=2}^{\infty} P_{3h} \cdot \cos(3h\omega t - \varphi_{3h}) \tag{5}$$

where:

$$P_{3h} = 3V_s \sqrt{I_{L(3h-1)}^2 + I_{L(3h+1)}^2 + 2I_{L(3h-1)} I_{L(3h+1)} \cos(\varphi_{3h+1} - \varphi_{3h-1})} \tag{6}$$

and

$$\tan\varphi_{3h} = \frac{I_{L(3h+1)} \sin\varphi_{3h+1} + I_{L(3h-1)} \sin\varphi_{3h-1}}{I_{L(3h+1)} \cos\varphi_{3h+1} + I_{L(3h-1)} \cos\varphi_{3h-1}} \tag{7}$$

The instantaneous power drawn by the non-linear load is:

$$p_L(t) = P_L + \tilde{p}_L(t) \tag{8}$$

where P_L is the active power used by the non-linear load and $\tilde{p}_L(t)$ is the instantaneous fluctuant/distortion power due to the same non-linear load.

$$P_L = 3 \cdot V_s \cdot I_{L1} \cdot \cos\varphi_1 \tag{9}$$

After compensation the instantaneous power delivered by the supply is:

$$p_s = [v_s]^t \cdot [i_s] = P_s = 3 \times V_s \times I_s \tag{10}$$

where P_s is the dc component of p_s *(t)* and represents the active power delivered by the supply.

The instantaneous power transferred through the active converter is:

$$p_c(t) = p_L(t) - P_s + P_o = P_L - P_s + \tilde{p}_L(t) = P_c + \tilde{p}_c(t) \tag{11}$$

where P_o is the active power delivered to dc bus.

But: $P_c = P_L - P_s + P_o$ (12)

Therefore: $\tilde{p}_c(t) = \tilde{p}_L(t)$ (13)

In steady state, the fluctuating power $\tilde{p}_c(t)$ at the output of active converter compensates the fluctuating power of the non-linear load. Equation (13) expresses the power exchange between the supply, non-linear load and active converter. If the losses in the ***H*** converter are neglected, then the fluctuating power $\tilde{p}_c(t)$ is converted into the ripple voltage $\tilde{v}_o(t)$ across the condenser. When a transient change in the active power demanded by the load occurs, the storage element (C) should be capable of compensating this unbalance. This results in a variation of the dc bus voltage. If the active power delivered by the source was inferior to the load demand ($P_c > 0$), then the average (V_o) voltage across the capacitor decreases. If the load demands less active power ($P_s < 0$), then V_o increases. The variation of the dc bus is compensated by the voltage regulator [8].

IV. POWER QUALITY IMPROVEMENT

As presented above, the active converter handles the fluctuating power that occurs in the load. Then, the main problem was to prove that the active converter simultaneously perform the necessary functions for power quality improvement. Into the decentralized strategy promoted by this study, the main function of the front-end stage should be as unity power factor rectifier.

For the purpose of this study, the following parameters have been chosen: V_o = 700 V, I_o = 20A, C = 1000μF, L = 1mH, r = 1mΩ, V_s = 220 V_{rms}/phase; Matlab 6 has been used as simulation tool.

A. UPFR and Reactive Compensation

For this situation, the phase-load current I_{L1} was 57.3 A_{rms} with a phase-shift of 24.3^0; this gives a power factor of 0.91 lagging. The result of compensation is as shown in figure 4.

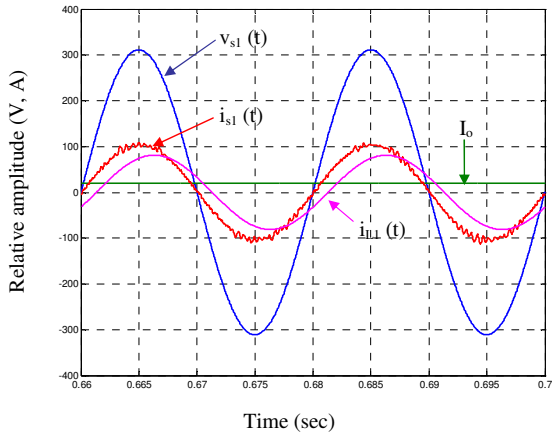

Fig. 4. UPFR and Reactive Compensation

From the above figure it is observed that the supply current (I_{s1} = 74.1 A_{rms}) is in phase with the voltage while the main function is still performed.

B. UPFR and Harmonic Compensator

A very non-linear load current of I_{L1} = 27.3 A_{rms} with THD of 127% and 10.6^0 fundamental-phase-shift was considered. As a result of compensation, using the proposed strategy, the load current (i_{L1}), dc current delivered (I_o), supply voltage (v_{s1}) and supply current (i_{s1}) are as in Fig. 5.

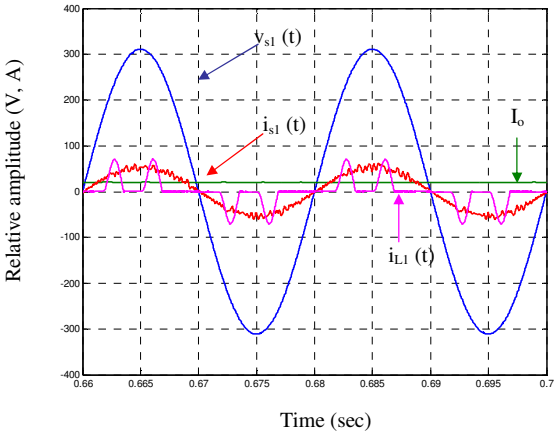

Fig. 5. UPFR and Harmonic Compensation

Figure 6 shows the spectrum of load (non-linear) current while figure 7 shows the spectrum of supply current and the improvement in total harmonic distortion (THD) to 6%.

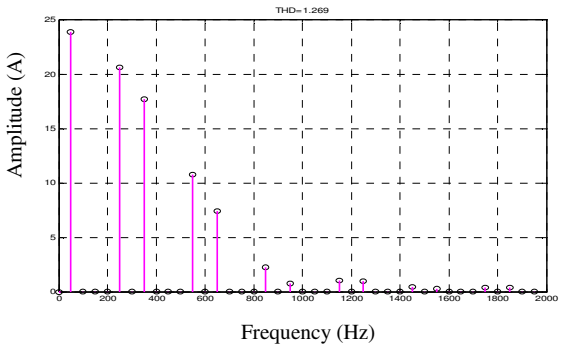

Fig. 6. Frequency spectrum of load (non-linear) current

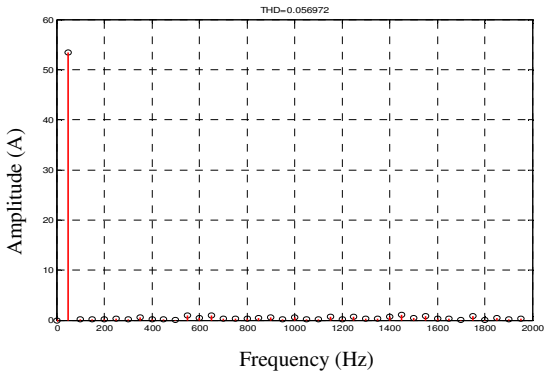

Fig. 7. Frequency spectrum of supply current after compensation

C. UPFR and APF

In this case, the currents from the previous paragraphs have been added resulting in a load current of I_{L1} = 75 A_{rms} with a THD of 29.8% and a fundamental phase-shift of approximately -16.5^0. The result of compensation is shown in figure 8; it is noticed that the shape and phase-shift of the supply current have improved.

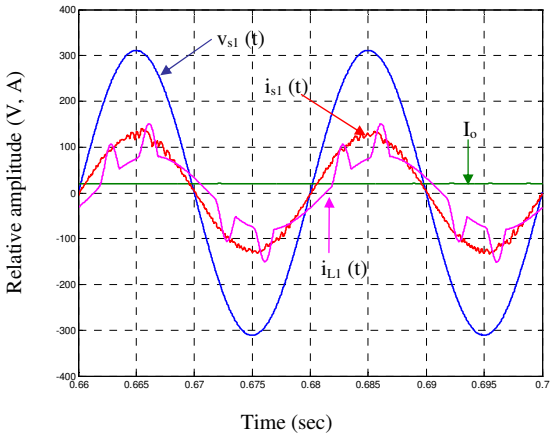

Fig. 8. UPFR and APF

Figure 9 shows the frequency spectrum of load (non-linear) current and figure 10 shows harmonic compensation of the supply current with a THD of approximately 4%.

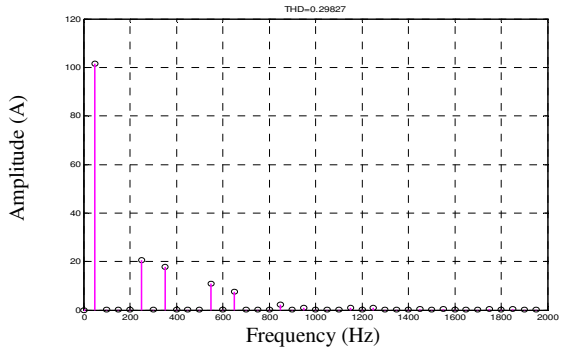

Fig. 9. Frequency spectrum of load (non-linear) current

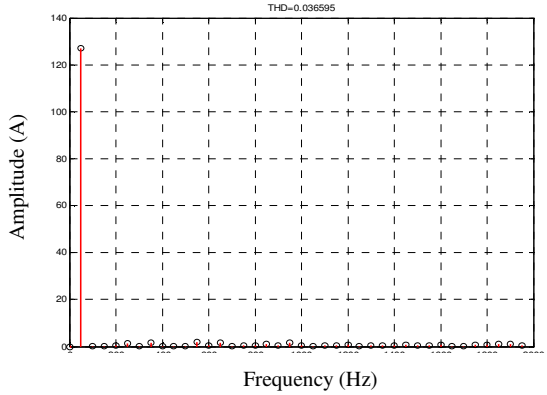

Fig. 10. Frequency spectrum of supply current

D. UPFR and Unbalanced Load

For this particular situation, a source impedance of 0.5 mH & 0.5 mΩ was considered. The load current system (see figure 11) was: I_{L1} = 44.8 A_{rms} (with a phase-shift of φ ≈ 27^0 and THD ≈ 3.5%), I_{L2} = 58.1 A_{rms} (with a phase-shift of φ ≈ 24^0 and THD ≈ 3.8%) and I_{L3} = 71.9 A_{rms} (with a phase-shift of φ ≈ 24^0 and THD ≈ 3%); this represents an unbalance of 48 % approximately. Without compensation, these currents have an influence in the voltage supply such as: V_{s1} = 216.4 V (with a THD of 1%), V_{s2} = 215.4 V (with a THD of 1.4%) and V_{s3} = 214.1 V (with a THD of 1.4%); this represents an unbalance of 7.4 % approximately.

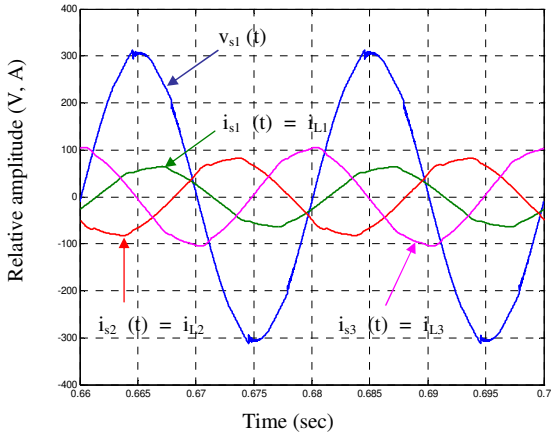

Fig. 11. Unbalanced current system

After compensation (figure 12), the supply current system becomes: I_{s1} = 70.2 A_{rms} (with a phase-shift of φ ≈ 1.8^0 and THD ≈ 2.6%), I_{s2} = 73.6 A_{rms} (with a phase-shift of φ ≈ 1^0 and THD ≈ 2.6%) and I_{s3} = 80.7 A_{rms} (with a phase-shift of φ ≈ 1^0 and THD ≈ 2.1%); this represents an unbalance of 26 % approximately. The voltage supply system becomes: V_{s1} = 216 V, V_{s2} = 215.8 V and V_{s3} = 215.4 V; this represents an unbalance of 3.7 % approximately.

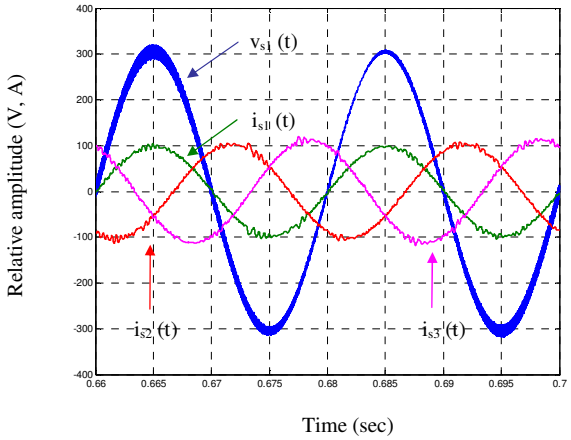

Fig. 12. UPFR & unbalancing compensation

From figure 12 one can notice the improvement not only in balancing the current system but also the reactive and harmonic compensation.

V. DYNAMIC COMPENSATION

Results so far present static situations. The behavior of the front-end active converter in a dynamic situation may be investigated by considering the case when one load current dropped suddenly by 30%.

Figure 13 shows the dynamic compensation. Dash lines show the load currents while solid lines indicate the source currents. It is observed that after the dynamic change in the load current, the source current system is still well balanced.

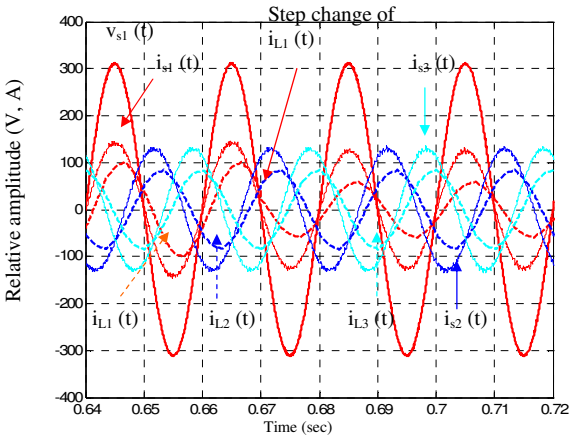

Fig. 13. Dynamic compensation for unbalanced current system

Figure 14 shows the dynamic compensation when the harmonic distortion of the load current suddenly increased from 8.1 % to 10.5%. As can be noticed the supply current keeps a low harmonic content of 1.7%, which compares well as the pre-sudden-change value of 1.5%.

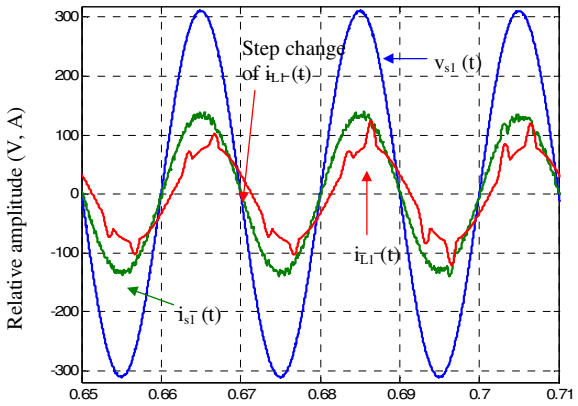

Fig. 14. Dynamic compensation for change in harmonic content

VI. MAXIMUM DEMAND SMOOTHING

As shown in figure 15, in any distribution system, the daily load curve presents a peak that must be flattened if possible. One main task of the distributed power conditioning is to deliver a certain amount of power during the peak demand.

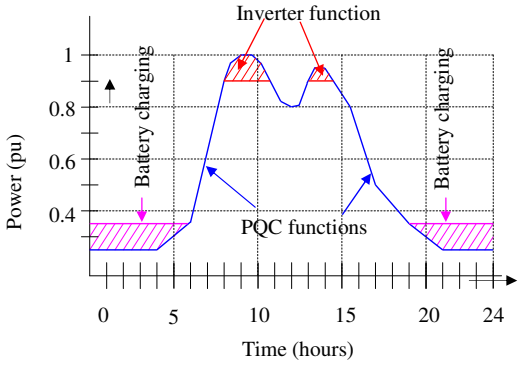

Fig. 15. Daily load curve & proposed strategy

The front-end stage proposed in this study can perform the inverter function introducing a back-up battery. No major alterations of the controller are required: the current loop stays unchanged, only the voltage loop is going to be modified. The initiation and duration of the inverter function depends on the capacity of the battery and it's charging status.

Figure 16 shows the influence of the inverter function on the supply current per phase.

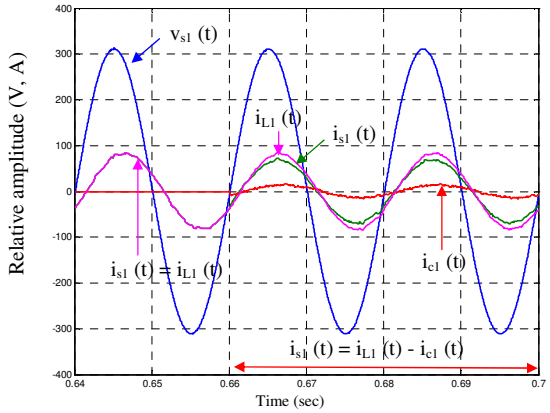

Fig. 16. Impact of inverter function

VII. SOME DESIGN CRITERIA

The relation between the components of the current: active (i_a), reactive (i_r) and non-linear (i_n – harmonic content) was another aspect studied in this paper. Generally, the current can be written as:

$$i(t) = i_a(t) + i_r(t) + i_n(t) \tag{14}$$

$$i_a(t) = \left(I_1 \cos\varphi_1\right)\sin\omega t \tag{15}$$

$$i_r(t) = \left(I_1 \sin\varphi_1\right)\cos\omega t \tag{16}$$

$$i_n(t) = \sum_{h=3,5,7,\ldots}^{\infty} I_{nh} \sin\left(h\omega t - \varphi_h\right) \tag{17}$$

where I_1 is the magnitude of the fundamental and I_{nh} is the harmonic of h order.

For each of these currents we can associate a phasor. Two phasors are orthogonal if the scalar product is nil [11]. Using the definition of the scalar product and equations (15) to (17), it is possible to find that:

$$\overline{i_a \cdot i_r} = 0 \tag{18}$$

$$\overline{i_a \cdot i_h} = 0 \tag{19}$$

$$\overline{i_r \cdot i_h} = 0 \tag{20}$$

If three phasors are orthogonal to each other, then they can be represented as the sides of a rectangular parallelepiped. For the current components in phase with the voltage but also for the orthogonal components, the superposition principle is applicable.

Based on the simulation results from previous paragraphs, the orthogonal relation among the three components of the current will be shown. The rms value of the current will be used: I_{sr} - rms supply current, I_{Lr} - rms load current, I_{dr} - rms output converter current, I_{cr} - rms input converter/filter current and I_o - dc output current. The values of these current for different situations presented in paragraphs IV.A, IV.B and IV.C are shown in table 1.

TABLE 1. RMS SYSTEM CURRENTS

	I_{L1}			I_{cr} (A)	I_o (A)	I_{s1}		I_{dr}	
	Magn. (A)	Phase (^{0})	THD (%)			Meas. (A)	Estim. (A)	Meas. (A)	Estim. (A)
IV.*A*	57.3	-24.3	0	33.3	20	74.1	73.4	32.3	31.7
IV.*B*	27.3	10.6	127	31.5	20	38.8	37.8	31.2	30.6
IV.*C*	74.9	-16.5	29.8	37.7	20	90.4	90	37.4	36.9

Taking into consideration the power balance, the superposition principle, and that various components of the current are orthogonal, the following relations could be found:

$$I_{sr} = \frac{I_{Lr} \times \cos\varphi}{\sqrt{1+THD^2}} + I_{or}\frac{V_o}{3\times V_{sr}} \tag{21}$$

$$I_{dr}^2 = \frac{I_{Lr}^2 \times \sin^2\varphi}{1+THD^2} + I_{Lr}^2\frac{THD^2}{1+THD^2} + \left(I_{or}\frac{V_o}{3\times V_{sr}}\right)^2 \tag{22}$$

As one can notice the accuracy of the estimated values using equations (21) and (22) is fairly good; the errors are mainly due to switching ripple.

Once the maximum phase-shift and THD are determined for the specific implementation place of this PQC method, then the ratings of the front-end IGBTs can be determined. After the ratings of the transistors have been determined, the maximum capability for maximum demand smoothing can be found; but this is also related with the back-up battery.

VII. CONCLUSIONS

In this paper a new strategy of power quality improvement and maximum demand smoothing has been presented. This method is suitable in many industrial and non-industrial applications.

The simultaneity of the main functions that contribute to power quality improvement has been presented. This proves that reactive power, harmonics and voltage unbalancing can be automatically addressed with the front end stage proposed to be introduced in devices which need an ac-to-dc conversion. Also some design criteria necessary for the implementation of the strategy have been shown.

The implementation of this method could minimize the capital investment and the cost of it can be recovered faster due to maximum demand smoothing.

VIII. REFERENCES

[1] T.G. Wilson, "The Evolution of Power Electronics", IEEE Transaction on Industrial Applications, Vol. 32, No. 6, 1996

[2] R.P Bingham, D. Kreises, and S. Santoso, *Advances in data reduction techniques for power quality instrumentation*. In Proc. Third European Power Quality Conf. Power Quality, Bremen, Germany, Nov. 1995**.**

[3] C.Y. Lee, *Effect of unbalanced voltage on the operation performance of a three-phase induction motor*, IEEE Trans. Energy Conv., vol. 14, pp. 202-208, June 1999

[4] H. Akagi, "The State-of-Art of Power Electronics in Japan"**,** IEEE Transactions On Power Electronics, Vol. 13, No. 2, March 1998

[5] H. Akagi, "New trends in active filters for power conditioning"**,** IEEE Transactions On Industrial Applications, Vol. 32, No. 6, 1996

[6] P. Ladoux, "Correction du Facteur de Puissance", Journees Strategies de Depollution Harmonique des Reseaux Electrique, Saint Nazaire, France, April 2000, pp161-170

[7] A.D. le Roux, J.A. du Toit, J.H.R. Enslin, "Integrated Active Rectifier and Power Quality Compensator with Reduced Current Measurement", IEEE Transactions On Industrial Electronics, Vol. 46, No. 3, June 1999

[8] D.V. Nicolae and M.J. Case, *Generalized Voltage Control for a Multi-Purpose Switching-Mode Converter*, "EPE-PEMC 2002", Dubrovnik / Croatia, September 2002

[9] J.-C. Le Claire, S. Siala, J Saillard, R. Le Doeuff, "Novel analog modulator for PWM control of alternative currents", Revue International de Genie Electrique, Vol.3, No.1/2000,pp 109-131

[10] D.V. Nicolae, I. Hofsajer and I.R. Jandrell, *Power Transfer through Multi-Purpose Switching-Mode Converters,* "IEEE Bologna Power Tech 2003 Conference", Bologna, Italy, June 2003

[11] J.H.R. Enslin, "Determination and dynamic compensation of fictious power in electric power systems", PhD Thesis, RAU, Johannesburg, June 1988